

Instance-Based Transfer Learning with Similarity-Aware Subject Selection for Cross-Subject SSVEP-Based BCIs

Ziwen Wang¹, Yue Zhang², Zhiqiang Zhang³, Sheng Quan Xie³, Alexander Lanzon¹, William P. Heath⁴, and Zhenhong Li¹

¹University of Manchester ²University of Bath ³University of Leeds ⁴Bangor University

Abstract—Steady-state visual evoked potential (SSVEP)-based brain-computer interfaces (BCIs) can achieve high recognition accuracy with sufficient training data. Transfer learning presents a promising solution to alleviate data requirements for the target subject by leveraging data from source subjects; however, effectively addressing individual variability among both target and source subjects remains a challenge. This paper proposes a novel transfer learning framework, termed instance-based task-related component analysis (iTRCA), which leverages knowledge from source subjects while considering their individual contributions. iTRCA extracts two types of features: (1) the subject-general feature, capturing shared information between source and target subjects in a common latent space, and (2) the subject-specific feature, preserving the unique characteristics of the target subject. To mitigate negative transfer, we further design an enhanced framework, subject selection-based iTRCA (SS-iTRCA), which integrates a similarity-based subject selection strategy to identify appropriate source subjects for transfer based on their task-related components (TRCs). Comparative evaluations on the Benchmark, BETA, and a self-collected dataset demonstrate the effectiveness of the proposed iTRCA and SS-iTRCA frameworks. This study provides a potential solution for developing high-performance SSVEP-based BCIs with reduced target subject data.

Index Terms—Brain-computer interface, steady-state visual evoked potential, transfer learning, negative transfer, cross-subject recognition, subject selection.

I. INTRODUCTION

SSVEP-based brain-computer interfaces (BCIs) facilitate direct communication between the brain and external devices [1]. They have been widely used in robotics [2]–[4], rehabilitation [5]–[8], and entertainment [9] due to their high information transfer rate (ITR), high signal-to-noise ratio (SNR), noninvasiveness, and minimal training needs [10], [11].

Precise decoding of steady-state visual evoked potential (SSVEP) from electroencephalogram (EEG) signals is crucial for SSVEP-based BCIs. Existing methods can be broadly categorized into training-free (e.g., [12], [13]) and training-based approaches (e.g., [14]–[19]). Compared to training-free approaches, training-based approaches usually achieve higher accuracy, provided that sufficient training data is collected during the calibration process, which is often time-consuming and labor-intensive.

Cross-subject transfer learning offers a potential solution to alleviate data requirements for the target subject (i.e., the new subject whose SSVEP signals need to be recognized) by transferring knowledge from source subjects (i.e., subjects whose data have been previously collected). Existing transfer learning approaches fall into two categories: one-to-one and all-to-one approaches. The one-to-one approach transfers knowledge from each source subject to the target subject individually and integrates the results using a grand average to form the final recognition criterion. Examples include inter and intra-subject maximal correlation (IISMC) [20], domain generalization-based transfer learning (DGTF) [21] and one-to-one cross-subject TRCA in [22]. The all-to-one approach, by contrast, constructs a unified representation of all source subjects through grand averaging, then transfers knowledge based on this integrated representation. Examples include transfer-related component analysis (TransRCA) [23], all-to-one cross-subject TRCA in [22], intra- and inter-subject CCA (IISCCA) [24] and cross-subject spatial filter transfer (CSSFT) [25]. However, the grand average in one-to-one and all-to-one approaches both implicitly assume equal contributions from all source subjects during transfer, overlooking the substantial variability across source subjects. To address this, the pioneering algorithm in [26] assigns contribution scores to source subjects in the final recognition criterion based on normalized correlation coefficients. However, these coefficients are assigned after knowledge transfer, and how to account for the varying contributions of source subjects during knowledge transfer remains an open problem.

Furthermore, not all source subjects contribute positively to the target subject's SSVEP recognition [27], [28]. When the knowledge learned from source subjects have a detrimental effect on the target subject (e.g., reducing recognition accuracy), the transfer is regarded as negative transfer [29]. To mitigate this phenomenon, pioneering work has begun to develop subject selection strategies prior to transfer, which generally follow a two-step approach: (1) evaluate each source subject's transferability based on recognition accuracy; (2) select several top-performing subjects to transfer, e.g. CSSFT [25], accuracy-based subject selection (ASS) [24], and subject transferability estimation (STE) [11]. However, these accuracy-based selection strategies require a complete recognition process for each source subject prior to transfer learning, imposing

TABLE I: Datasets Description

Dataset	Benchmark	BETA	Self-collected
Subjects	35 healthy subjects (17F / 18M)	70 healthy subjects (28F / 42M)	11 healthy subjects (5F / 6M)
Stimuli	40 stimuli $f_i = 8 + 0.2(i - 1)$ Hz, $i = 1, 2, \dots, 40$.	40 stimuli $f_i = 8 + 0.2(i - 1)$ Hz, $i = 1, 2, \dots, 40$.	12 stimuli $f_i = 9.25 + 0.5(i - 1)$ Hz, $i = 1, 2, \dots, 12$.
Trials	40 trials / 6 blocks	40 trials / 4 blocks	12 trials / 5 blocks
Time	0.5 s cue + 5 s flickering + 0.5 s rest	0.5 s cue + 2 s or 3 s flickering + 0.5 s rest	0.5 s cue + 5 s flickering + 0.5 s rest

computational load and extended processing time [24].

In this paper, we propose a new transfer learning framework, instance-based task-related component analysis (iTRCA), for cross-subject SSVEP recognition. Motivated by the private-share component analysis in neural network design [30], iTRCA innovatively employs a dual-feature approach that combines both the general characteristics across subjects and the unique characteristics of the target subject.

- 1) Subject-general feature: this feature captures the general characteristics of SSVEP response across source and target subjects through transfer learning. During the transfer learning, we innovatively formulate each source subject's SSVEP response as an instance and construct a common latent space between source instances and the target subject, considering different contributions of source instances. In this space, the source instances and the target subject's SSVEP response are maximally correlated.
- 2) Subject-specific feature: this feature captures the individual characteristics of the target subject's SSVEP response based on task-related component analysis (TRCA).

To avoid negative transfer, we further propose a similarity-based subject selection strategy to filter out source instances that are dissimilar to the target. Different from the existing subject selection strategies, the proposed strategy quantifies the similarity based on subjects' task-related components (TRCs), thereby eliminating the need for a complete recognition process for each source subject. Comparative studies are carried out on three datasets: Benchmark, BETA, and a self-collected dataset, and evaluated against state-of-the-art methods TransRCA [23], DGTF [21], and CSSFT [25]. The results demonstrate the superior recognition performance of iTRCA compared to baseline methods, and further enhanced through the integration of subject selection strategy. Additionally, our proposed similarity-based subject selection strategy substantially reduces computational cost compared to the accuracy-based method.

II. METHODS

A. Dataset

In this study, three datasets were utilized: two public datasets (Benchmark [31] and BETA [32]) generated by Tsinghua University, and a self-collected dataset generated by the University of Leeds. Essential details about three datasets are summarized in Table I.

Fig. 1 illustrates the experiment paradigm of the self-collected dataset. The interaction interface was composed of

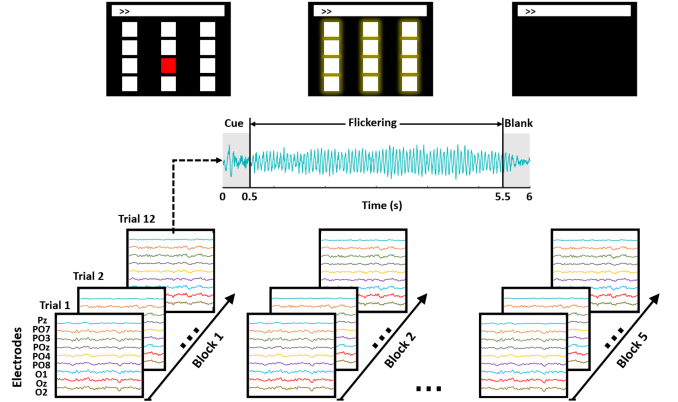


Fig. 1: The experiment paradigm of the self-collected dataset.

12 flickering stimuli arranged in a 4×3 matrix and displayed on the 23.6-inch LCD monitor with a resolution of 1920×1080 pixels and a refresh rate of 60 Hz. The stimuli were encoded using joint frequency and phase modulation (JFPM) approach [33], where frequencies varied from 9.25 Hz to 14.75 Hz in 0.5 Hz increments and phase shifts cycled from 0π to 1.5π in 0.5π increments. The experiment consisted of 5 blocks, each containing 12 trials corresponding to different stimuli. Each trial began with a 0.5 s red dot cue indicating the target flicker, followed by 5 s of gaze fixation on the target, and concluded with 0.5 s of rest before the next trial. EEG signals were recorded at 256 Hz using g.USBamp (g.tec medical engineering) and then band-pass filtered between 8 and 40 Hz using the IIR filter of Chebyshev type I. The experiment was approved by the Research Ethics Committee of the University of Leeds (reference number MEEC 21-024), and all participants signed the informed consent. To ensure consistency in data processing, the signals from Benchmark and BETA datasets were band-pass filtered between 8 Hz and 88 Hz using the IIR filter of Chebyshev type I.

Across all three datasets, nine electrodes located in parietal and occipital areas (Pz, PO7, PO3, POz, PO4, PO8, O1, O2, and O2) were employed for three datasets. EEG signals were segmented within the window $[0.64, 0.64 + d]$ s, accounting for the 0.5 s gaze shifting and 0.14 s latency delay, where d denotes the data length used for SSVEP recognition.

B. Notations

For each subject, the multi-channel EEG signals are denoted by a 4-th order tensor. For source subjects, the available

training data are represented by

$$\{\mathcal{X}^{S_n} \in \mathbb{R}^{N_f \times N_c \times N_s \times N_{sb}}\}_{n=1}^{N_{src}}$$

with entries $\mathcal{X}^{S_n}(i, p, q, h) \in \mathbb{R}$, where n and N_{src} denote the index and total number of source subjects, respectively. For the target subject, the available training data are represented by

$$\mathcal{X}^{T_a} \in \mathbb{R}^{N_f \times N_c \times N_s \times N_{tb}}$$

with entries $\mathcal{X}^{T_a}(i, p, q, j) \in \mathbb{R}$. The indices and dimensions of tensors are defined as follows:

- i and N_f : The index and total number of stimuli.
- p and N_c : The index and total number of channels.
- q and N_s : The index and total number of samples.
- h and N_{sb} : The index and total number of source blocks.
- j and N_{tb} : The index and total number of target blocks.

For simplicity, we will use the source subject's tensor \mathcal{X}^{S_n} as an example to introduce the definition of notation. For the n -th source subject and i -th stimulus, a single trial in the h -th block is denoted as the 2-D matrix $\mathbf{X}_{i,h}^{S_n} = \mathcal{X}^{S_n}(i, :, :, h) \in \mathbb{R}^{N_c \times N_s}$, trials from all blocks are denoted as $\mathbf{X}_i^{S_n} = \mathcal{X}^{S_n}(i, :, :, :) \in \mathbb{R}^{N_c \times N_s \times N_{sb}}$, the individual template is the grand average across all blocks, i.e., $\bar{\mathbf{X}}_i^{S_n} = 1/N_{sb} \sum_{h=1}^{N_{sb}} \mathbf{X}_{i,h}^{S_n} \in \mathbb{R}^{N_c \times N_s}$, and their ground truth label is the visual stimulus frequency f_i . These rules of notation definition also apply to the target subject's tensor \mathcal{X}^{T_a} .

In this study, we consider N_f visual stimuli at frequencies f_1, f_2, \dots, f_{N_f} . Given a test trial $\tilde{\mathbf{X}} \in \mathbb{R}^{N_c \times N_s}$ from the target subject, we aim to recognize the corresponding stimulus frequency $\hat{f} \in \{f_1, f_2, \dots, f_{N_f}\}$, using both training data from the target subject \mathcal{X}^{T_a} and source subjects $\{\mathcal{X}^{S_n}\}_{n=1}^{N_{src}}$.

C. iTRCA

iTRCA is a transfer learning framework for SSVEP cross-subject recognition, incorporating both subject-general and subject-specific features. Inspired by the concept of instance-based transfer learning [34], iTRCA computes the TRCs of source subjects as source instances and then projects them into a latent space, where these source instances and the target subject's template exhibit maximal correlation. This latent space captures the underlying characteristics of SSVEP responses shared between source and target subjects, while accounting for the varying contributions of individual source subjects. Meanwhile, iTRCA captures target subject's individual characteristics using TRCA. The overall framework is illustrated in Fig. 2 and includes following steps.

1) *Compute the source instances*: TRC, which is the single-channel signal spatially filtered from multi-channel EEG signal based on TRCA [19], is chosen as the instance of each source subject due to its low-dimensional nature and demonstrated effectiveness in recovering SSVEP characteristics [23], [35].

For the n -th source subject and i -th stimulus, the spatial filter $\mathbf{w}_i^{S_n} \in \mathbb{R}^{N_c}$ is invariant across different trials. First, the spatially filtered inter-trial covariance across all combinations is summed together

$$\begin{aligned} & \sum_{\substack{h_1, h_2=1 \\ h_2 \neq h_1}}^{N_{sb}} \text{Cov} \left((\mathbf{w}_i^{S_n})^\top \mathbf{X}_{i,h_1}^{S_n}, (\mathbf{w}_i^{S_n})^\top \mathbf{X}_{i,h_2}^{S_n} \right) \\ &= \sum_{\substack{h_1, h_2=1 \\ h_2 \neq h_1}}^{N_{sb}} (\mathbf{w}_i^{S_n})^\top \text{Cov}(\mathbf{X}_{i,h_1}^{S_n}, \mathbf{X}_{i,h_2}^{S_n}) \mathbf{w}_i^{S_n} \\ &= (\mathbf{w}_i^{S_n})^\top \mathbf{S}_i^{S_n} \mathbf{w}_i^{S_n}, \end{aligned} \quad (1)$$

where

$$\mathbf{S}_i^{S_n} = \sum_{\substack{h_1, h_2=1 \\ h_2 \neq h_1}}^{N_{sb}} \text{Cov}(\mathbf{X}_{i,h_1}^{S_n}, \mathbf{X}_{i,h_2}^{S_n}). \quad (2)$$

Then, the variance of the spatially filtered signal is constrained to 1

$$\begin{aligned} & \sum_{h=1}^{N_{sb}} \text{Cov} \left((\mathbf{w}_i^{S_n})^\top \mathbf{X}_{i,h}^{S_n}, (\mathbf{w}_i^{S_n})^\top \mathbf{X}_{i,h}^{S_n} \right) \\ &= \sum_{h=1}^{N_{sb}} (\mathbf{w}_i^{S_n})^\top \text{Cov}(\mathbf{X}_{i,h}^{S_n}, \mathbf{X}_{i,h}^{S_n}) \mathbf{w}_i^{S_n} \\ &= (\mathbf{w}_i^{S_n})^\top \mathbf{Q}_i^{S_n} \mathbf{w}_i^{S_n} \\ &= 1, \end{aligned} \quad (3)$$

where

$$\mathbf{Q}_i^{S_n} = \sum_{h=1}^{N_{sb}} \text{Cov}(\mathbf{X}_{i,h}^{S_n}, \mathbf{X}_{i,h}^{S_n}). \quad (4)$$

The spatial filter $\mathbf{w}_i^{S_n}$ is computed by maximizing (1) under the constraint (3), which is in the form of Rayleigh Quotient [36]

$$\hat{\mathbf{w}}_i^{S_n} = \arg \max_{\mathbf{w}_i^{S_n}} \frac{(\mathbf{w}_i^{S_n})^\top \mathbf{S}_i^{S_n} \mathbf{w}_i^{S_n}}{(\mathbf{w}_i^{S_n})^\top \mathbf{Q}_i^{S_n} \mathbf{w}_i^{S_n}}. \quad (5)$$

Therefore, the optimal spatial filter can be solved as the eigenvector of matrix $(\mathbf{Q}_i^{S_n})^{-1} \mathbf{S}_i^{S_n}$ corresponding to the largest eigenvalue. For simplicity, the calculation of $\hat{\mathbf{w}}_i^{S_n}$ from (1) to (5) is defined as the following function

$$\hat{\mathbf{w}}_i^{S_n} = \text{TRCA}(\mathbf{X}_i^{S_n}), \quad (6)$$

where the input $\mathbf{X}_i^{S_n}$ represents all training trials for the n -th source subject and i -th stimulus. The single-channel TRC $\mathbf{y}_i^{S_n}$ is extracted from the individual template $\bar{\mathbf{X}}_i^{S_n}$

$$\mathbf{y}_i^{S_n} = (\hat{\mathbf{w}}_i^{S_n})^\top \bar{\mathbf{X}}_i^{S_n} \in \mathbb{R}^{1 \times N_s}. \quad (7)$$

The TRCs from all source subjects are vertically concatenated as the source template,

$$\mathbf{Y}_i^S = \begin{bmatrix} \mathbf{y}_i^{S_1} \\ \mathbf{y}_i^{S_2} \\ \vdots \\ \mathbf{y}_i^{S_{N_{src}}} \end{bmatrix} \in \mathbb{R}^{N_{src} \times N_s}, \quad (8)$$

which is the unified representation of source subjects.

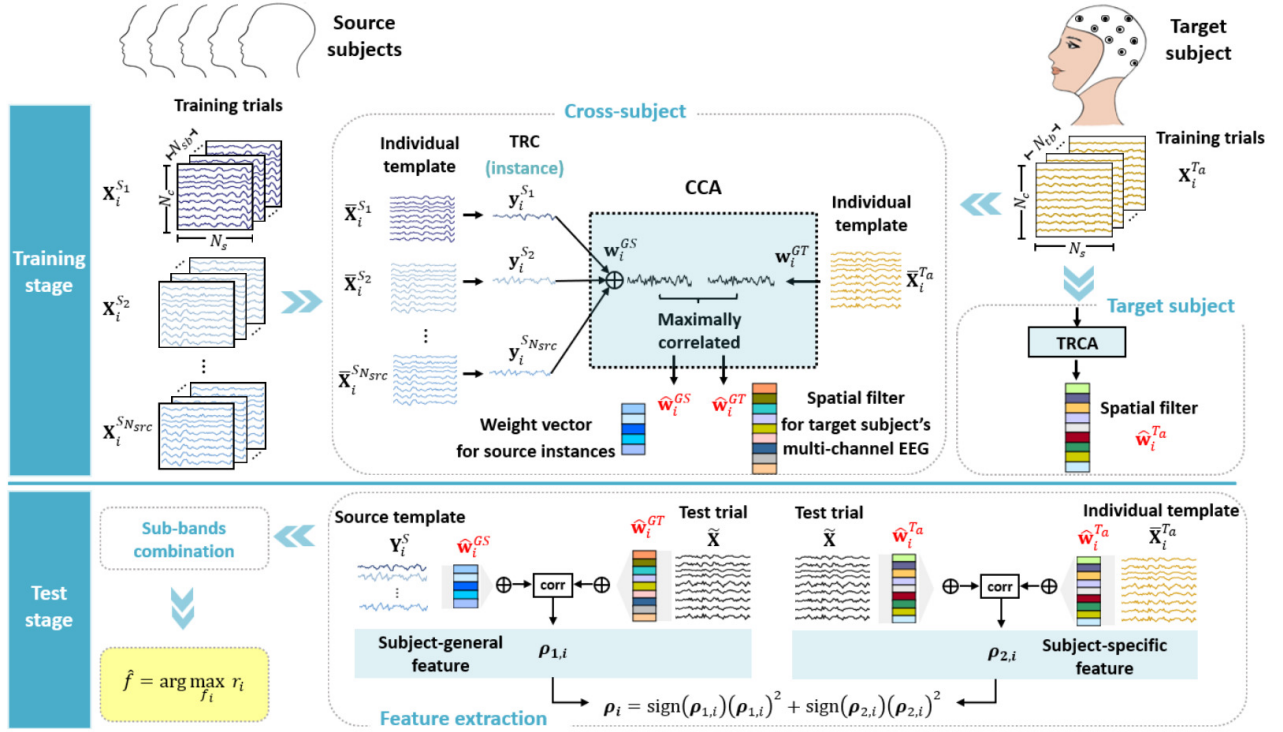


Fig. 2: Diagram of the proposed iTRCA framework. For the i -th stimulus, the shared information across subjects is captured in a common latent space (the blue block) where source instances and the target subject's individual template are maximally correlated through weight vector $\hat{\mathbf{w}}_i^{GS}$ and the spatial filter $\hat{\mathbf{w}}_i^{GT}$. Meanwhile, target subject's individual information is captured by the spatial filter $\hat{\mathbf{w}}_i^{Ta}$ based on TRCA. In the test stage, the feature ρ_i is composed of the subject-general feature $\rho_{1,i}$ and the subject-specific feature $\rho_{2,i}$, and then combined across all sub-bands to formulate the feature r_i used for SSVEP recognition.

2) *Weight source instances*: For the i -th stimulus, the source template \mathbf{Y}_i^S and the target subject's individual template $\bar{\mathbf{X}}_i^{Ta} = 1/N_{tb} \sum_{j=1}^{N_{tb}} \mathbf{X}_{i,j}^{Ta} \in \mathbb{R}^{N_c \times N_s}$ are projected to a common latent space where they are maximally correlated by the source weight vector $\hat{\mathbf{w}}_i^{GS} \in \mathbb{R}^{N_{src}}$ and the target spatial filter $\hat{\mathbf{w}}_i^{GT} \in \mathbb{R}^{N_c}$ based on canonical correlation analysis (CCA) [37] as follows:

$$[\hat{\mathbf{w}}_i^{GS}, \hat{\mathbf{w}}_i^{GT}] = \arg \max_{\mathbf{w}_i^{GS}, \mathbf{w}_i^{GT}} \text{corr}((\mathbf{w}_i^{GS})^\top \mathbf{Y}_i^S, (\mathbf{w}_i^{GT})^\top \bar{\mathbf{X}}_i^{Ta}), \quad (9)$$

where $\text{corr}(\cdot, \cdot)$ is Pearson correlation.

3) *Feature extraction*: iTRCA extracts two kinds of features: subject-general and subject-specific features. Given a test trial $\tilde{\mathbf{X}}$ from the target subject, the subject-general feature for the i -th stimulus is formulated as

$$\rho_{1,i} = \text{corr}((\hat{\mathbf{w}}_i^{GT})^\top \tilde{\mathbf{X}}, (\hat{\mathbf{w}}_i^{GS})^\top \mathbf{Y}_i^S). \quad (10)$$

The subject-specific feature is extracted by TRCA

$$\rho_{2,i} = \text{corr}((\hat{\mathbf{w}}_i^{Ta})^\top \tilde{\mathbf{X}}, (\hat{\mathbf{w}}_i^{Ta})^\top \bar{\mathbf{X}}_i^{Ta}), \quad (11)$$

where $\hat{\mathbf{w}}_i^{Ta} = \text{TRCA}(\bar{\mathbf{X}}_i^{Ta})$. The final feature is integrated as

$$\rho_i = \text{sign}(\rho_{1,i})(\rho_{1,i})^2 + \text{sign}(\rho_{2,i})(\rho_{2,i})^2. \quad (12)$$

Subject-general feature is the correlation between the spatially filtered test trial and the weighted source template, measuring the similarity between the test trial and shared

information in the common latent space constructed by $\hat{\mathbf{w}}_i^{GT}$ and $\hat{\mathbf{w}}_i^{GS}$. Subject-specific feature is the correlation between the spatially filtered test trial and the target subject's TRC, measuring the similarity between the test trial and the target subject's individual information. Incorporating both, the final feature balances the shared information and individual information of the test trial.

4) *Filter bank analysis*: Not only is the fundamental frequency useful for the SSVEP, but the harmonic components also contribute significantly [38]. To take advantage of harmonic components, the SSVEP signals are decomposed into multiple sub-band components using the M_3 method in [39], and features are calculated individually for each sub-band based on (12). All sub-band features are then combined to enhance recognition performance.

The index of the sub-band is denoted by m , and the total number is N_m . For the i -th stimulus, the combined feature across sub-bands is given by

$$r_i = \sum_{m=1}^{N_m} \alpha(m) \rho_i^{(m)}, \quad (13)$$

where the coefficient $\alpha(m) = m^{-1.25} + 0.25$. The stimulus frequency of the test trial can be recognized by the combined feature

$$\hat{f} = \arg \max_{f_i} r_i, \quad i = 1, 2, \dots, N_f. \quad (14)$$

D. Subject selection-based iTRCA (SS-iTRCA)

To mitigate negative transfer, a subject selection strategy is developed to select a subset of source subjects \mathcal{S} which are more similar to the target subject prior to transfer learning. In this preliminary step, each source subject is assigned a similarity coefficient c_i^n that quantifies the correlation between the target TRC and the source TRC

$$c_i^n = \text{corr}(\mathbf{x}_i^{T_a}, \mathbf{y}_i^{S_n}), \quad n = 1, 2, \dots, N_{src}, \quad (15)$$

where $\mathbf{x}_i^{T_a} = (\hat{\mathbf{w}}_i^{T_a})^T \bar{\mathbf{X}}_i^{T_a}$.

The subject selection module is governed by the trigger parameter γ . If $c_i^n \leq \gamma, \forall n \in \{1, 2, \dots, N_{src}\}$, it indicates that all source subjects exhibit relatively low similarity to the target subject. In this case, the subject selection module is disabled as we prefer to have more data rather than selecting subjects from a less similar group, thereby all source subjects are included for transfer

$$\mathcal{S} = \{n | n \in \{1, 2, \dots, N_{src}\}\}. \quad (16)$$

Otherwise, if $\exists n \in \{1, 2, \dots, N_{src}\}$ such that $c_i^n > \gamma$, the selection mechanism is triggered. The normalized similarity value \tilde{c}_i^n is defined as

$$\tilde{c}_i^n = \frac{|c_i^n|}{c_i^{max}}, \quad (17)$$

where

$$c_i^{max} = \max\{|c_i^1|, |c_i^2|, \dots, |c_i^{N_{src}}|\}. \quad (18)$$

The normalized similarity \tilde{c}_i^n lies within the range $[0, 1]$. As \tilde{c}_i^n approaches 1, the source subject is more closely related to the target subject. Source subjects with \tilde{c}_i^n exceeding the lower boundary $c_{lb} \in [0, 1]$ are selected for transfer

$$\mathcal{S} = \{n | \tilde{c}_i^n > c_{lb}, n \in \{1, 2, \dots, N_{src}\}\}. \quad (19)$$

Integrating the subject selection module, iTRCA framework is extended to SS-iTRCA. Note that the proposed subject selection is based on TRC, which has already been computed in iTRCA. This design avoids redundant calculations and reduces the additional computational cost introduced by subject selection.

The SS-iTRCA framework can transition to iTRCA and TRCA by adjusting the parameter c_{lb} . When $c_{lb} = 0$, the set of selected source subjects would be

$$\begin{aligned} \mathcal{S} &= \{n | \tilde{c}_i^n > 0, n \in \{1, 2, \dots, N_{src}\}\} \\ &= \{n | n \in \{1, 2, \dots, N_{src}\}\}. \end{aligned} \quad (20)$$

All source subjects are included, thereby SS-iTRCA transitions to iTRCA framework. As c_{lb} increases, the stricter similarity threshold is applied, resulting in fewer source subjects being selected. Since $\max(\tilde{c}_i^1, \tilde{c}_i^2, \dots, \tilde{c}_i^{N_{src}}) = 1$, we will have at least one source subject selected when $0 \leq c_{lb} < 1$. When $c_{lb} = 1$, the set of selected source subjects would be

$$\begin{aligned} \mathcal{S} &= \{n | \tilde{c}_i^n > 1, n \in \{1, 2, \dots, N_{src}\}\} \\ &= \emptyset. \end{aligned} \quad (21)$$

Here, no source subjects are selected, meaning that only the target subject's data is used, thereby SS-iTRCA transitions to TRCA method.

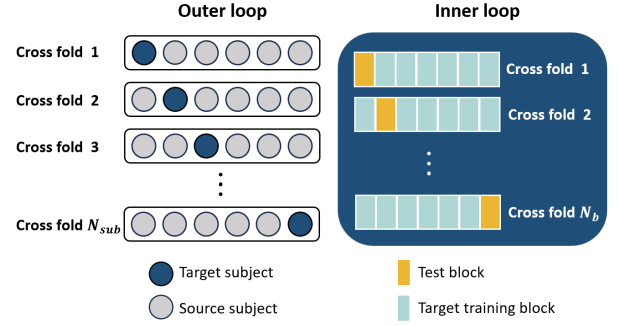


Fig. 3: The illustration of leave-one-subject-out and leave-one-block-out cross-validation strategies.

E. Evaluations

The proposed iTRCA and SS-iTRCA are evaluated in both public datasets (Benchmark and BETA) and the self-collected dataset, as described in Section II-A. Accuracy and ITR are utilized to evaluate the SSVEP recognition performance. The ITR (bits/min) represents the amount of information communicated per unit time [1] and can be calculated by

$$\text{ITR} = \left(\log_2 N_f + P \log_2 P + (1 - P) \log_2 \frac{1 - P}{N_f - 1} \right) \frac{60}{T}, \quad (22)$$

where P is the classification accuracy and T is the time in seconds for a selection which implies the data length of signals for recognizing a stimulus, including both the gaze shifting (0.5 s) and gaze time.

We utilize leave-one-out cross-validation strategies for evaluation shown in Fig. 3. This strategy defines how the dataset is systematically partitioned for training and testing, involving two parameters inherent to the dataset: N_{sub} , the total number of subjects in the dataset, and N_b , the total number of blocks for each subject in the dataset.

In the outer loop, leave-one-subject-out (LOSO) cross-validation is applied to split the target subject and source subjects. Each subject in the dataset is iteratively treated as the target subject, while the remaining subjects serve as source subjects, i.e., $N_{src} = N_{sub} - 1$. All blocks from each source subject are used for training, i.e., $N_{sb} = N_b$. In the inner loop, leave-one-block-out (LOBO) cross-validation is applied for the target subject. In this step, each block (highlighted in orange) is iteratively selected as the test block, while a subset of the remaining blocks is used for training, i.e., $N_{tb} \leq N_b - 1$. Consequently, the recognition performance of each target subject is evaluated across all blocks, and the overall performance is assessed across all subjects.

This section evaluates the recognition performance of iTRCA and SS-iTRCA over TRCA with respect to d , N_c , and N_{tb} on three datasets.

III. RESULTS

To assess transfer performance, the proposed frameworks iTRCA and SS-iTRCA are compared to TRCA method focusing on recognition accuracy, ITR, and feature distribution. Additionally, the effect of subject selection is investigated

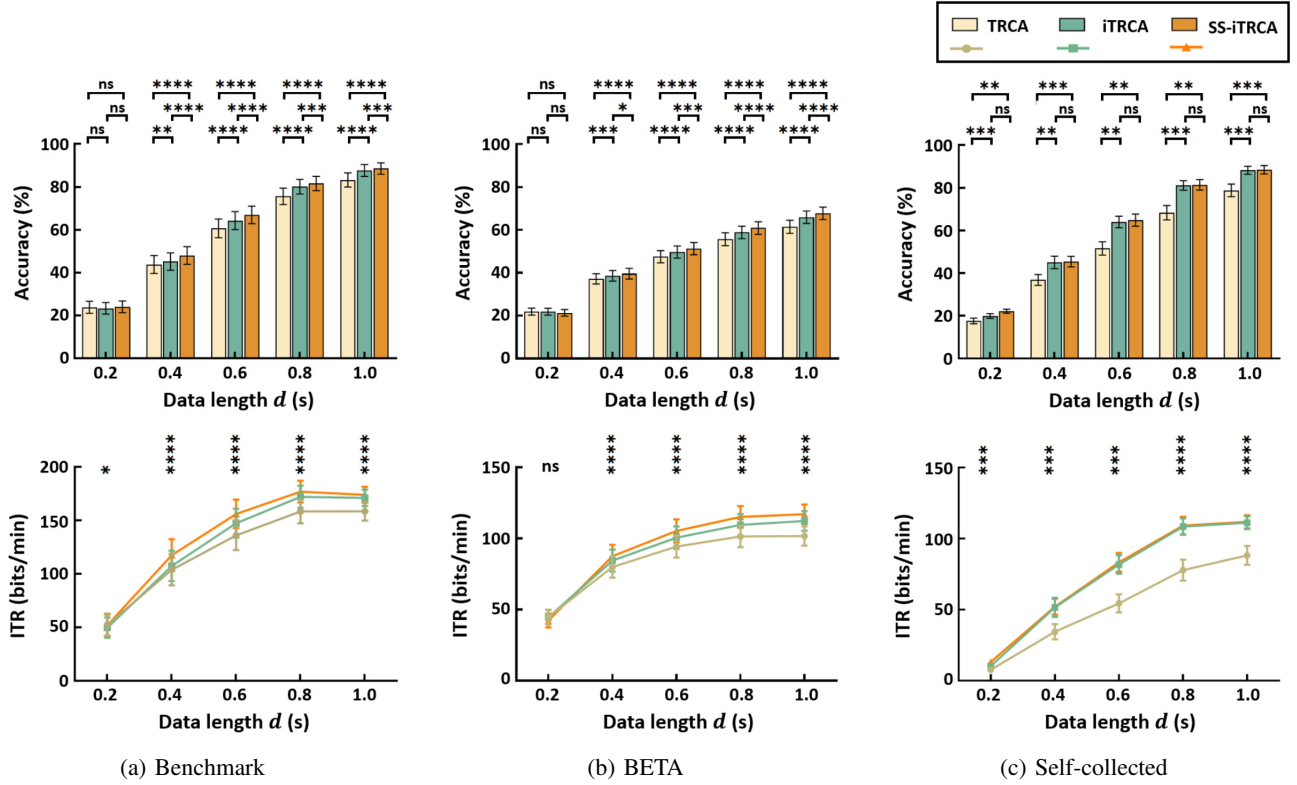


Fig. 4: The average recognition accuracy and ITR for TRCA, iTRCA and SS-iTRCA across all subjects for different d on three datasets: (a) Benchmark, (b) BETA, and (c) Self-collected. Error bars represent stand error of mean (SEM). Asterisks indicate the statistically significant difference between two algorithms (* : $p < 0.05$, ** : $p < 0.01$, *** : $p < 0.001$, **** : $p < 0.0001$). Accuracy and ITR are analyzed by two-way and one-way repeated-measures ANOVA, respectively.

through a comparative analysis between iTRCA and SS-iTRCA. Finally, the proposed transfer learning frameworks are examined against existing transfer learning methods TransRCA, DGTF, and CSSFT. The evaluation parameters include:

- data length d ;
- the number of channels N_c ;
- the number of target blocks N_{tb} ;
- lower boundary of similarity c_{lb} (for subject selection).

Each parameter is analyzed independently, with the others held constant. In this study, all available blocks in the dataset are used as source blocks, i.e., $N_{sb} = N_b$. In the filter bank analysis, the number of sub-band components N_m is set to 3 and applied across all datasets.

A. Recognition performance

Fig. 4 shows the average accuracy and ITR across all subjects for d ranging from 0.2 s to 1 s in 0.2 s increments, with $N_c = 9$, $N_{tb} = 3$, and $c_{lb} = 0.9$. Across all datasets, recognition accuracy of all algorithms increases monotonically with d , suggesting that longer data segments provide more reliable information for recognition when $d < 1$ s. On public datasets (Benchmark and BETA), iTRCA outperforms TRCA from 0.4 s onward, with SS-iTRCA further improving accuracy. However, the extent of improvement varies: on BETA, SS-iTRCA shows a more pronounced accuracy enhancement over iTRCA as d increases, whereas on Benchmark, the

accuracy difference is less significant. On the self-collected dataset, iTRCA consistently outperforms TRCA across all d values, while SS-iTRCA achieves comparable accuracy to iTRCA, with no statistically significant differences observed.

Regarding ITR, the results across all datasets show a consistent pattern: ITR increases rapidly from 0.2 s to 0.6 s, peaks around 0.8 s, and either stabilizes or slightly declines at 1 s. Unlike the monotonic increase in accuracy, ITR exhibits a growth-and-decline trend as d increases, reflecting the trade-off between recognition speed and accuracy: longer d enhances accuracy but also reduces speed, potentially lowering overall transfer efficiency. On public datasets, SS-iTRCA achieves the highest ITR from 0.4 s onward, TRCA the lowest, and iTRCA lies in between. On the self-collected dataset, SS-iTRCA and iTRCA show comparable ITR performance, while TRCA consistently lags behind across all d values.

Fig. 5 presents the average accuracy across all subjects for N_c ranging from 3 to 9, with $d = 1$ s, $N_{tb} = 3$, and $c_{lb} = 0.9$. Nine EEG electrodes in the occipital region (highlighted in orange in Fig. 5d) are arranged as Pz, PO7, PO3, POz, PO4, PO8, O1, Oz, and O2. The first N_c electrodes are used to analyze spatial patterns; for example, when $N_c = 5$, Pz, PO7, PO3, POz, and PO4 are utilized for analysis. Across all datasets, SS-iTRCA consistently achieves the highest accuracy, followed by iTRCA, with TRCA significantly lower. The difference between SS-iTRCA and iTRCA is most pronounced on BETA and statistically significant on Benchmark, while

TABLE II: Recognition Accuracy (%) for Different Number of Target Blocks N_{tb}

N_{tb}	Benchmark			BETA			Self-collected		
	TRCA	SS-iTRCA	Δ	TRCA	SS-iTRCA	Δ	TRCA	SS-iTRCA	Δ
2	71.06	82.38	11.32	49.59	58.67	9.08	61.52	82.70	21.19
3	83.23	88.56	5.29	61.43	67.73	6.30	78.75	88.41	9.66
4	88.01	91.24	3.22	–	–	–	87.42	90.45	3.03
5	90.64	92.86	2.21	–	–	–	–	–	–

Δ is the accuracy difference between SS-iTRCA and TRCA.

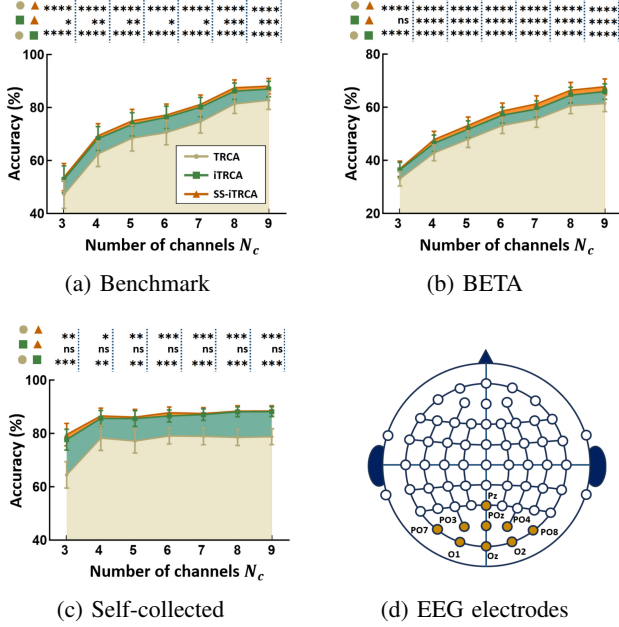


Fig. 5: The average recognition accuracy for TRCA, iTRCA and SS-iTRCA across all subjects for different N_c on three datasets: (a) Benchmark, (b) BETA, and (c) Self-collected. The nine EEG electrodes utilized in this study are highlighted in orange in (d).

no significant difference is observed on the self-collected dataset. Regarding the sensitivity to N_c , accuracy consistently improves as N_c increases from 3 to 9 on Benchmark and BETA, but shows minimal improvement beyond 4 channels on the self-collected dataset.

Fig. 6 exhibits the average recognition accuracy for N_{tb} ranging from 2 to $N_b - 1$ ($N_b = 6, 4,$ and 5 in Benchmark, BETA, and self-collected dataset, respectively), with $d = 1$ s, $N_c = 9$, and $c_{lb} = 0.9$. Across three datasets, the recognition accuracy of all algorithms increases monotonically as N_{tb} increases, demonstrating that the target subject's recognition accuracy benefits from more of their own training data. On public datasets (Benchmark and BETA), SS-iTRCA achieves the highest accuracy, followed by iTRCA, while TRCA performs the worst. On the self-collected dataset, TRCA remains the lowest, with iTRCA and SS-iTRCA showing comparable accuracy and no statistically significant differences. The accuracy gap among SS-iTRCA, iTRCA, and TRCA follows a consistent trend across three datasets as N_{tb} increases: the gap

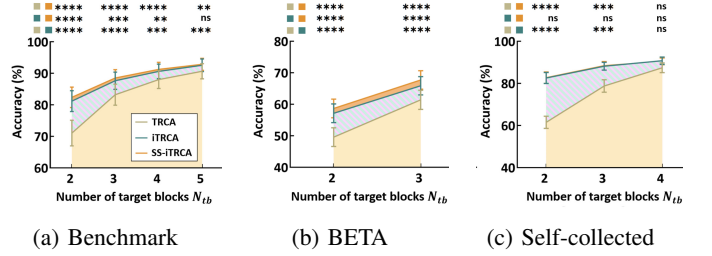


Fig. 6: The average recognition accuracy for TRCA, iTRCA and SS-iTRCA across all subjects at different N_{tb} on three datasets.

between SS-iTRCA and iTRCA remains steady, while the gap between iTRCA and TRCA is most pronounced at $N_{tb} = 2$ and gradually narrows. The difference values are organized in Table II. When $N_{tb} = 2$, Δ reaches 11.32%, 9.08%, and 21.19% on Benchmark, BETA, and the self-collected dataset, corresponding to relative improvements of 15.93%, 18.31%, and 34.44%. These results highlight the effectiveness of proposed transfer learning frameworks in scenarios with scarce target subject data.

Comprehensively evaluating Figs.4-6, iTRCA and SS-iTRCA consistently achieve higher accuracy across various experimental conditions (d , N_c , and N_{tb}), as summarized in Table III. On average, iTRCA and SS-iTRCA improve accuracy by 4.65% and 5.87% over d , 6.07% and 7.18% over N_c , and 7.35% and 8.17% over N_{tb} , demonstrating their superior capability to leverage auxiliary data from source subjects for more accurate SSVEP recognition.

B. Feature distribution

Fig. 7 illustrates the ability of recognition algorithm distinguishing features from different stimuli. The extracted features based on (13) are reduced from high-dimensional space (40D for Benchmark and BETA, 12D for the self-collected dataset) to a 2D space using the t-distributed stochastic neighbor embedding (t-SNE) technique [40], with $d = 0.6$ s, $N_c = 9$, $N_{tb} = 3$, and $c_{lb} = 0.9$.

The CHI [41] is employed to assess clustering performance as the ratio of between-cluster dispersion to within-cluster dispersion, with higher CHI values indicating better clustering performance. Across all datasets, it is observed that the clusters become more compact and well-separated from the left figure (TRCA) to the right (SS-iTRCA), reflected in higher CHI val-

TABLE III: Recognition Accuracy (%) Comparison

Parameter	Benchmark			BETA			Self-collected		
	TRCA	iTRCA	SS-iTRCA	TRCA	iTRCA	SS-iTRCA	TRCA	iTRCA	SS-iTRCA
d	57.38	60.07	61.78	44.73	46.97	48.15	50.61	59.62	60.41
N_c	69.64	74.93	76.00	50.66	54.48	55.98	76.45	85.56	86.33
N_{tb}	83.24	88.01	88.75	55.51	61.52	63.20	75.90	87.16	87.19

Note: the accuracy is the average value across all cases.

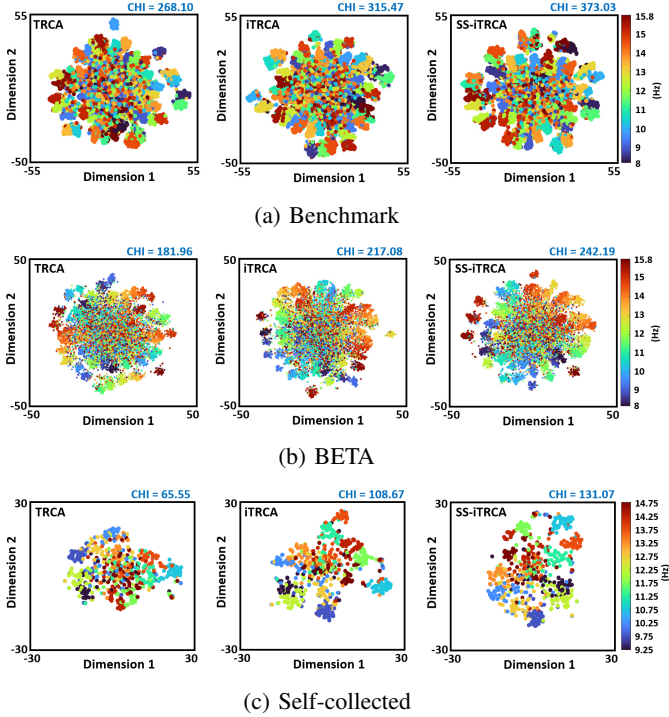


Fig. 7: t-SNE visualization on (a) Benchmark, (b) BETA, and (c) Self-collected dataset. Each point represents a reduced 2D feature for a single trial out of $N_f \times N_b \times N_{sub}$ total trials, where N_{sub} and N_b refer to the iterations of LOSO and LOBO cross-validation, respectively. Each stimulus includes $N_b \times N_{sub}$ trials, represented by distinct colors as shown in the color bar. Calinski-Harabasz Index (CHI) values are displayed in the upper-right corner of each figure to evaluate clustering performance.

ues, indicating progressive improvements in clustering quality. Comparing performance across datasets, the clusters are tighter and more distinct on Benchmark, moderately separable on BETA, and less separable on the self-collected data.

C. Subject selection

The number of selected source subjects is determined by the selection trigger (γ) and similarity lower boundary (c_{lb}). In this study, we set the trigger $\gamma = 0.5$ and examine the effect of c_{lb} on recognition accuracy and the number of selected source subjects on the Benchmark dataset, with $d = 0.6$ s, $N_c = 9$, and $N_{tb} = 3$.

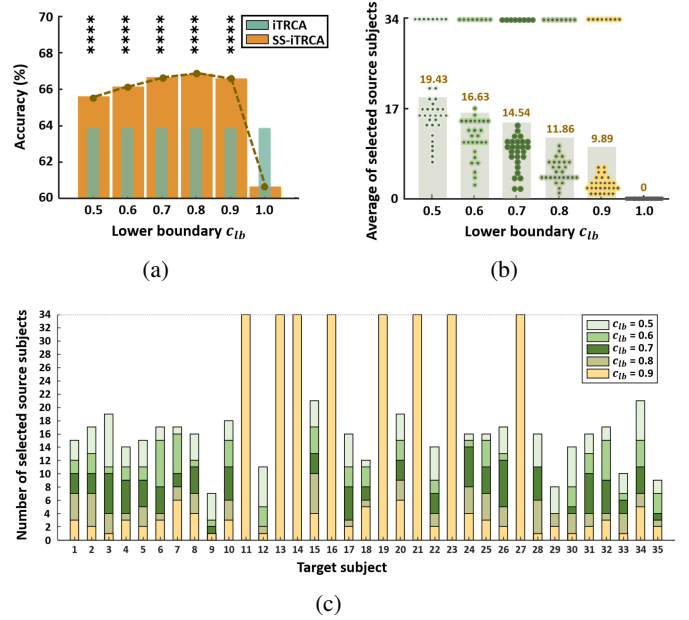


Fig. 8: Subject selection performance on Benchmark. (a) Average recognition accuracy across all subjects. (b) The number of selected source subjects where the scatter point represents the target subject and the gray bar represents the average number across 35 target subjects. (c) The number of selected source subjects for each target subject at different thresholds c_{lb} . For example, for target subject 1, the number of selected source subjects is 15, 12, 10, 7, and 3 at $c_{lb} = 0.5, 0.6, 0.7, 0.8$, and 0.9 , respectively. For target subject 11, all source subjects are included, corresponding to the case described in (16), where the subject selection strategy is not triggered.

Fig. 8a shows the average recognition accuracy across all subjects for iTRCA and SS-iTRCA, with c_{lb} ranging from 0.5 to 1. Since iTRCA is unaffected by c_{lb} , its accuracy remains constant across all c_{lb} values. In contrast, the accuracy of SS-iTRCA gradually increases as c_{lb} rises, peaking at 0.8 before slightly declining and ultimately reducing to TRCA at $c_{lb} = 1$, as discussed in (21). Fig. 8b illustrates the average number of selected source subjects as c_{lb} varies, demonstrating that increasing c_{lb} tightens selection criteria, leading to fewer source subjects being selected.

D. Comparison with existing transfer learning method

In this subsection, we further evaluate the proposed frameworks SS-iTRCA and iTRCA against state-of-the-art transfer

learning methods, TransRCA [23], DGTF [21], and CSSFT [25]. Leave-one-out cross-validation strategies are employed across all methods, as described in section II-E. Fig. 9a presents the average recognition accuracy across all subjects for d varying from 0.2 s to 1 s, with $N_c = 9$, $N_{tb} = 3$, and $c_{lb} = 0.9$ on the benchmark dataset. The proposed frameworks consistently outperforms TransRCA, DGTF, and CSSFT across all d values, with statistically significant differences.

Fig. 9b illustrates the average training and inference time with $d = 1$ s. All experiments are conducted using MATLAB R2022a on a Windows 11 system, equipped with a 13th Intel Core i7-13700H CPU running at 2.40 GHz and an NVIDIA GeForce RTX 4070 Laptop GPU. For both training and inference stages, SS-iTRCA, iTRCA and TransRCA exhibit significantly lower computational costs compared to CSSFT and DGTF. Although TransRCA achieves shorter training time than SS-iTRCA and iTRCA, there is no statistically significant difference in inference time among them, which is crucial for real-time signal recognition. Compared with accuracy-based subject selection method CSSFT, the proposed similarity-based subject selection strategy SS-iTRCA substantially reduces the computation cost.

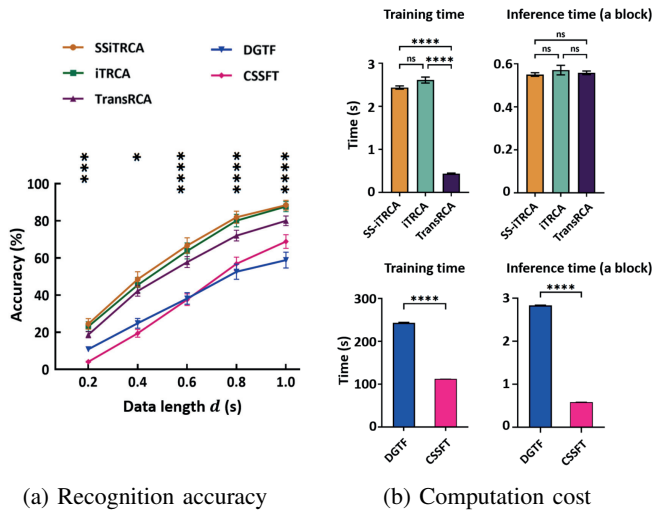


Fig. 9: Performance comparison between the proposed methods (SS-iTRCA and iTRCA) with existing transfer learning methods (TransRCA, DGTF, and CSSFT). (a) Recognition accuracy, with a paired t-test conducted between iTRCA and TransRCA. (b) Training and inference time for each method, where the test time corresponds to a block comprising 40 test trials in the benchmark dataset.

Comprehensively, the proposed SS-iTRCA and iTRCA frameworks demonstrate superior recognition performance with comparable inference time. In addition, the designed similarity-based subject selection strategy substantially enhances computational efficiency relative to accuracy-based method.

IV. DISCUSSION

A. Transfer learning performance

Section III-A demonstrates the capability of proposed transfer learning frameworks (iTRCA and SS-iTRCA) to leverage auxiliary data from the source subjects to improve the SSVEP recognition, over the conventional TRCA. Internally, these improvements stem from the quality of extracted features, as demonstrated in Section III-B. Features extracted by iTRCA and SS-iTRCA exhibit a more compact distribution for the same stimulus across subjects and greater separation for different stimuli, with higher CHI values than TRCA. This indicates the enhanced ability of iTRCA and SS-iTRCA to handle inter-subject variability, a common challenge in SSVEP-based BCI systems.

The advantages of our transfer learning framework are more pronounced with limited training data from the target subject. As indicated by bold values in Table II, SS-iTRCA reaches higher accuracy than TRCA with one fewer training block, suggesting its promise as a solution for minimizing training data needs without compromising recognition accuracy.

Furthermore, the robustness of the iTRCA and SS-iTRCA is validated across three distinct cross-subject scenarios represented by different datasets. The Benchmark dataset (35 subjects, aged 17–34) serves as a standard for assessing cross-subject generalization performance. The BETA dataset (70 subjects, aged 9–64) captures a broad range of age groups and cognitive variability, which is essential for evaluating robustness across a heterogeneous population. The self-collected dataset (11 subjects) offers a smaller and more controlled setup to test adaptability in limited data scenarios. Across all datasets, iTRCA and SS-iTRCA consistently outperform TRCA, demonstrating their versatility and effectiveness in handling diverse cross-subject scenarios.

B. Subject selection-based transfer learning

SS-iTRCA is the enhanced framework of iTRCA with similarity-based subject selection. Figs. 4-7 consistently shows the superior performance of SS-iTRCA than iTRCA on public datasets (Benchmark and BETA), while their performance is comparable without statistically significant differences on the self-collected dataset. This can be attributed to the small sample size (11 subjects). Under this condition, if we continue to reduce source subjects, the transfer model would struggle to extract generalized information from limited data, even if they are more similar to the target subject. This aligns with the finding from Fig. 8a, which suggests a balance between the similarity and the number of transferred subjects.

Additionally, Fig. 8a reveals the occurrence of negative transfer. As c_{lb} decreases ($c_{lb} \leq 0.8$), more source subjects with lower similarity to the target subject are included, leading to a decline in accuracy. This finding coincides with the negative transfer, where the dissimilar source data can hurt the target task [42] (target subject's SSVEP recognition in this study), highlighting the importance of source subject selection. Moreover, it demonstrates that the designed TRC-based metric (17) can reflect the similarity between source and target subjects, thereby improving recognition accuracy even

with fewer, but more relevant, source subjects. Fig. 8c shows how the subject selection mechanism behaves for different source subjects. It can be observed that when subjects 9 and 29 are chosen as target subjects, even when the similarity threshold is set to a low value $c_{tb} = 0.5$, only a few source subjects are selected. This indicates that the SSVEP responses of these target subjects are less similar (unique) in the sense of TRC. This uniqueness may be attributed to various factors, such as subject variability, inappropriate data processing, etc.

Finally, beyond improving accuracy, SS-iTRCA also significantly reduces computational cost compared to the accuracy-based CSSFT method (Fig. 9b), demonstrating the practical efficiency of similarity-based subject selection.

C. Limitations and future directions

While the proposed subject selection strategy performs well on public datasets (Benchmark and BETA), it does not demonstrate significant differences compared to not using it on the small-sample dataset, i.e., the self-collected dataset with 11 subjects. This limitation underscores the need for future research on effectively leveraging knowledge in source data-scarce scenarios.

In addition, deep learning-based transfer learning represents a promising future direction. However, it is important to note that the effectiveness of deep learning largely depends on the availability of large-scale training data, which still remains a challenge in EEG applications. Future studies should investigate how to adapt deep models to work efficiently under limited data conditions common in BCI scenarios.

V. CONCLUSION

In this study, we propose a transfer learning framework iTRCA that accounts for the differing contributions of source subjects, and an enhanced framework SS-iTRCA, which incorporates a novel subject-selection strategy. iTRCA and SS-iTRCA are evaluated on three datasets (Benchmark, BETA, and a self-collected dataset), consistently outperforming widely used TRCA method in recognition accuracy and feature distribution, particularly when target subject data is limited. Additionally, SS-iTRCA further enhances the performance of iTRCA and shows superior results compared to the existing transfer learning methods. These findings highlight iTRCA and SS-iTRCA as promising solutions for reducing target subject data requirements without compromising accuracy [43].

REFERENCES

- [1] J. R. Wolpaw, N. Birbaumer, D. J. McFarland, G. Pfurtscheller, and T. M. Vaughan, "Brain-computer interfaces for communication and control," *Clin. Neurophysiol.*, vol. 113, no. 6, pp. 767–791, Jun. 2002, doi:10.1016/S1388-2457(02)00057-3.
- [2] L. Shao, L. Zhang, A. N. Belkacem, Y. Zhang, X. Chen, J. Li, and H. Liu, "EEG-controlled wall-crawling cleaning robot using SSVEP-based brain-computer interface," *J. Healthc. Eng.*, vol. 2020, no. 1, p. 6968713, Jun. 2020, doi:10.1155/2020/6968713.
- [3] X. Chen, B. Zhao, Y. Wang, and X. Gao, "Combination of high-frequency ssvep-based bci and computer vision for controlling a robotic arm," *J. Neural Eng.*, vol. 16, no. 2, p. 026012, Feb. 2019, doi:10.1088/1741-2552/aaf594.
- [4] A. Chiuzbaian, J. Jakobsen, and S. Puthusserypadu, "Mind controlled drone: An innovative multiclass SSVEP based brain computer interface," in *Proc. 7th Int. Winter Conf. Brain-Comput. Interface (BCI)*, Gangwon, South Korea, 2019, pp. 1–5, doi:10.1109/IWW-BCI.2019.8737327.
- [5] P. G. Vinoy, S. Jacob, V. G. Menon, S. Rajesh, and M. R. Khosravi, "Brain-controlled adaptive lower limb exoskeleton for rehabilitation of post-stroke paralyzed," *IEEE Access*, vol. 7, pp. 132 628–132 648, Jun. 2019, doi:10.1109/ACCESS.2019.2921375.
- [6] X. Zhao, Y. Chu, J. Han, and Z. Zhang, "SSVEP-based brain-computer interface controlled functional electrical stimulation system for upper extremity rehabilitation," *IEEE Trans. Syst., Man, Cybern.: Syst.*, vol. 46, no. 7, pp. 947–956, May 2016, doi:10.1109/TSMC.2016.2523762.
- [7] R. Na, C. Hu, Y. Sun, S. Wang, S. Zhang, M. Han, W. Yin, J. Zhang, X. Chen, and D. Zheng, "An embedded lightweight SSVEP-BCI electric wheelchair with hybrid stimulator," *Digit. Signal Process.*, vol. 116, p. 103101, Sep. 2021, doi:10.1016/j.dsp.2021.103101.
- [8] A. Müller-Putz, R. Scherer, G. Pfurtscheller, and R. Rupp, "Control of an electrical prosthesis with an SSVEP-based BCI," *IEEE Trans. Biomed. Eng.*, vol. 55, no. 1, pp. 361–364, Dec. 2007, doi:10.1109/TBME.2007.897815.
- [9] Z. Wang, Y. Yu, M. Xu, Y. Liu, E. Yin, and Z. Zhou, "Towards a hybrid BCI gaming paradigm based on motor imagery and SSVEP," *Int. J. Hum.-Comput. Interact.*, vol. 35, no. 3, pp. 197–205, Mar. 2018, doi:10.1080/10447318.2018.1445068.
- [10] G. Bin, X. Gao, Y. Wang, B. Hong, and S. Gao, "VEP-based brain-computer interfaces: time, frequency, and code modulations [research frontier]," *IEEE Comput. Intell. Mag.*, vol. 4, no. 4, pp. 22–26, Oct. 2009, doi:10.1109/MCI.2009.934562.
- [11] H. Li, G. Xu, C. Du, Z. Li, C. Han, P. Tian, B. Li, and S. Zhang, "Facilitating applications of SSVEP-BCI by effective cross-subject knowledge transfer," *Expert Syst. Appl.*, vol. 249, p. 123492, Sep. 2024, doi:10.1016/j.eswa.2024.123492.
- [12] Y. Wang, R. Wang, X. Gao, B. Hong, and S. Gao, "A practical VEP-based brain-computer interface," *IEEE Trans. Neural Syst. Rehabil. Eng.*, vol. 14, no. 2, pp. 234–240, Jun. 2006, doi:10.1109/TNSRE.2006.875576.
- [13] Z. Lin, C. Zhang, W. Wu, and X. Gao, "Frequency recognition based on canonical correlation analysis for SSVEP-based BCIs," *IEEE Trans. Biomed. Eng.*, vol. 53, no. 12, pp. 2610–2614, Dec. 2006, doi:10.1109/TBME.2006.886577.
- [14] Y. Zhang, G. Zhou, Q. Zhao, A. Onishi, J. Jin, X. Wang, and A. Cichocki, "Multiway canonical correlation analysis for frequency components recognition in SSVEP-based BCIs," in *Proc. ICONIP*, Shanghai, China, 2011, pp. 287–295, doi:10.1007/978-3-642-24955-6_35.
- [15] G. Bin, X. Gao, Y. Wang, Y. Li, B. Hong, and S. Gao, "A high-speed BCI based on code modulation VEP," *J. Neural Eng.*, vol. 8, no. 2, p. 025015, Mar. 2011, doi:10.1088/1741-2560/8/2/025015.
- [16] Y. Zhang, G. Zhou, J. Jin, X. Wang, and A. Cichocki, "Frequency recognition in SSVEP-based BCI using multiset canonical correlation analysis," *Int. J. Neural Syst.*, vol. 24, no. 4, p. 1450013, Jun. 2014, doi:10.1142/S0129065714500129.
- [17] Y. Zhang, G. Zhou, J. Jin, M. Wang, X. Wang, and A. Cichocki, "L1-regularized multiway canonical correlation analysis for SSVEP-based BCI," *IEEE Trans. Neural Syst. Rehabil. Eng.*, vol. 21, no. 6, pp. 887–896, Oct. 2013, doi:10.1109/TNSRE.2013.2279680.
- [18] Y. Zhang, D. Guo, F. Li, E. Yin, Y. Zhang, P. Li, Q. Zhao, T. Tanaka, D. Yao, and P. Xu, "Correlated component analysis for enhancing the performance of SSVEP-based brain-computer interface," *IEEE Trans. Neural Syst. Rehabil. Eng.*, vol. 26, no. 5, pp. 948–956, Apr. 2018, doi:10.1109/TNSRE.2018.2826541.
- [19] M. Nakanishi, Y. Wang, X. Chen, Y.-T. Wang, X. Gao, and T.-P. Jung, "Enhancing detection of SSVEPs for a high-speed brain speller using task-related component analysis," *IEEE Trans. Biomed. Eng.*, vol. 65, no. 1, pp. 104–112, Apr. 2017, doi:10.1109/TBME.2017.2694818.
- [20] H. Wang, Y. Sun, F. Wang, L. Cao, W. Zhou, Z. Wang, and S. Chen, "Cross-subject assistance: Inter-and intra-subject maximal correlation for enhancing the performance of SSVEP-based BCIs," *IEEE Trans. Neural Syst. Rehabil. Eng.*, vol. 29, pp. 517–526, Feb. 2021, doi:10.1109/TNSRE.2021.3057938.
- [21] J. Huang, Z. Q. Zhang, B. Xiong, Q. Wang, B. Wan, F. Li, and P. Yang, "Cross-subject transfer method based on domain generalization for facilitating calibration of SSVEP-based BCIs," *IEEE Trans. Neural Syst. Rehabil. Eng.*, vol. 31, pp. 3307–3319, Aug. 2023, doi:10.1109/TNSRE.2023.3305202.
- [22] W. Liu, Y. Ke, P. Liu, J. Du, L. Kong, S. Liu, X. An, and D. Ming, "A cross-subject SSVEP-BCI based on task related component anal-

- ysis,” in *Proc. 41st EMBC*, Berlin, Germany, 2019, pp. 3022–3025, doi:10.1109/EMBC.2019.8857064.
- [23] W. Lan, R. Wang, Y. He, Y. Zong, Y. Leng, K. Iramina, W. Zheng, and S. Ge, “Cross domain correlation maximization for enhancing the target recognition of SSVEP-based brain-computer interfaces,” *IEEE Trans. Neural Syst. Rehabil. Eng.*, vol. 31, pp. 3545–3555, Aug. 2023, doi:10.1109/TNSRE.2023.3309543.
- [24] Q. Wei, Y. Zhang, Y. Wang, and X. Gao, “A canonical correlation analysis-based transfer learning framework for enhancing the performance of SSVEP-based BCIs,” *IEEE Trans. Neural Syst. Rehabil. Eng.*, vol. 31, pp. 2809–2821, Jun. 2023, doi:10.1109/TNSRE.2023.3288397.
- [25] W. Yan, Y. Wu, C. Du, and G. Xu, “Cross-subject spatial filter transfer method for SSVEP-EEG feature recognition,” *J. Neural Eng.*, vol. 19, no. 3, p. 036008, May 2022, doi:10.1088/1741-2552/ac6b57.
- [26] Y. Zhang, S. Q. Xie, C. Shi, J. Li, and Z. Q. Zhang, “Cross-subject transfer learning for boosting recognition performance in SSVEP-based BCIs,” *IEEE Trans. Neural Syst. Rehabil. Eng.*, vol. 31, pp. 1574–1583, Mar. 2023, doi:10.1109/TNSRE.2023.3250953.
- [27] S. J. Pan and Q. Yang, “A survey on transfer learning,” *IEEE Trans. Knowl. Data Eng.*, vol. 22, no. 10, pp. 1345–1359, Oct. 2009, doi:10.1109/TKDE.2009.191.
- [28] M. T. Rosenstein, Z. Marx, L. P. Kaelbling, and T. G. Dietterich, “To transfer or not to transfer,” in *NIPS 2005 workshop on transfer learning*, vol. 898, no. 3, 2005, p. 4.
- [29] K. Weiss, T. M. Khoshgoftaar, and D. Wang, “A survey of transfer learning,” *J. Big Data*, vol. 3, no. 9, pp. 1–40, May 2016, doi:10.1186/s40537-016-0043-6.
- [30] K. Bousmalis, G. Trigeorgis, N. Silberman, D. Krishnan, and D. Erhan, “Domain separation networks,” *Adv. Neural Inf. Process. Syst.*, vol. 29, 2016, doi:10.48550/arXiv.1608.06019.
- [31] Y. Wang, X. Chen, X. Gao, and S. Gao, “A benchmark dataset for SSVEP-based brain-computer interfaces,” *IEEE Trans. Neural Syst. Rehabil. Eng.*, vol. 25, no. 10, pp. 1746–1752, Nov. 2016, doi:10.1109/TNSRE.2016.2627556.
- [32] B. Liu, X. Huang, Y. Wang, X. Chen, and X. Gao, “BETA: A large benchmark database toward SSVEP-BCI application,” *Front. Neurosci.*, vol. 14, p. 627, Jun. 2020, doi:10.3389/fnins.2020.00627.
- [33] Y. Zhang, P. Xu, K. Cheng, and D. Yao, “Multivariate synchronization index for frequency recognition of SSVEP-based brain-computer interface,” *J. Neurosci. Methods*, vol. 221, pp. 32–40, Jan. 2014, doi:10.1016/j.jneumeth.2013.07.018.
- [34] J. Wang and Y. Chen, “Instance weighting methods,” in *Introduction to transfer learning: algorithms and practice*. Singapore: Springer Nature, 2023, pp. 67–77.
- [35] H. Tanaka, “Group task-related component analysis (gTRCA): A multivariate method for inter-trial reproducibility and inter-subject similarity maximization for EEG data analysis,” *Sci. Rep.*, vol. 10, no. 1, p. 84, Jan. 2020, doi:10.1038/s41598-019-56962-2.
- [36] R. A. Horn and C. R. Johnson, “Hermitian matrices, Symmetric matrices, and Congruences,” in *Matrix analysis*, 2nd ed. New York, USA: Cambridge Univ. Press, 2012, pp. 234–239.
- [37] K. V. Mardia, J. T. Kent, and C. C. Taylor, “Canonical Correlation Analysis,” in *Multivariate analysis*, 2nd ed. West Sussex, UK: John Wiley & Sons, 2024, pp. 281–293.
- [38] X. Chen, Y. Wang, M. Nakanishi, X. Gao, T.-P. Jung, and S. Gao, “High-speed spelling with a noninvasive brain-computer interface,” *Proc. Natl. Acad. Sci. U.S.A.*, vol. 112, no. 44, pp. E6058–E6067, Oct. 2015, doi:10.1073/pnas.1508080112.
- [39] X. Chen, Y. Wang, S. Gao, T.-P. Jung, and X. Gao, “Filter bank canonical correlation analysis for implementing a high-speed SSVEP-based brain-computer interface,” *J. Neural Eng.*, vol. 12, no. 4, p. 046008, Jun. 2015, doi:10.1088/1741-2560/12/4/046008.
- [40] L. Van der Maaten and G. Hinton, “Visualizing data using t-SNE,” *J. Mach. Learn. Res.*, vol. 9, pp. 2579–2605, Nov. 2008, [Online]. Available: <https://www.jmlr.org/papers/v9/vandermaaten08a.html>.
- [41] T. Caliński and J. Harabasz, “A dendrite method for cluster analysis,” *Commun. Stat. Theory Methods*, vol. 3, no. 1, pp. 1–27, Jun. 2007, doi:10.1080/03610927408827101.
- [42] Z. Wan, R. Yang, M. Huang, N. Zeng, and X. Liu, “A review on transfer learning in EEG signal analysis,” *Neurocomputing*, vol. 421, pp. 1–14, Jan. 2021, doi:10.1016/j.neucom.2020.09.017.
- [43] K.-J. Chiang, C.-S. Wei, M. Nakanishi, and T.-P. Jung, “Cross-subject transfer learning improves the practicality of real-world applications of brain-computer interfaces,” in *2019 9th International IEEE/EMBS Conference on Neural Engineering (NER)*. IEEE, 2019, pp. 424–427.